Solar Phys (2011) 272:91–100
DOI 10.1007/s11207-011-9812-8

Determination of Electron Density and Filling Factor for Soft X-Ray Flare Kernels

J. Jakimiec · U. Bąk-Stęślicka

Received: 23 November 2010 / Accepted: 25 May 2011 / Published online: 6 July 2011

Abstract In the standard method of electron density determination for soft X-ray (SXR) flare kernels, it is necessary to assume what the extent is of a kernel along the line of sight. This is a source of significant uncertainty of the obtained densities.

In our previous paper (Bąk-Stęślicka and Jakimiec, *Solar Phys.* **231**, 95, 2005) we have proposed a new method of deriving electron density, in which it is not necessary to assume what the extent of a kernel along the line of sight is. This new method is based on the idea that many flares, during their decay phase, can be described with a sequence of steady-state models [quasi-steady-state (QSS) evolution] and then a scaling law, derived for steady-state models, can be used to determine the electron density.

The aim of the present paper is: *i*) to improve both methods of density determination, and *ii*) to compare the densities obtained with the two methods. We have selected a number of flares which showed QSS evolution during their decay phase. For these flares the electron density, N, has been derived by means of both the standard method and with our QSS method. Comparison of the N values obtained with the two different methods allowed us: *i*) to test the obtained densities, *ii*) to evaluate the volume filling factor of the SXR emitting plasma.

Generally, we have found good agreement (no large systematic differences) between the values of electron density obtained with the two methods, though for some cases the values differed by up to a factor of two. For most flare kernels the filling factor turned out to be about one near the flare maximum.

Keywords Sun: corona · Flares · X-rays

J. Jakimiec · U. Bąk-Stęślicka (✉)
Astronomical Institute, University of Wrocław, ul. Kopernika 11, 51-622 Wrocław, Poland
e-mail: bak@astro.uni.wroc.pl

J. Jakimiec
e-mail: jjakim@astro.uni.wroc.pl

1. Introduction

Loop–top flare kernels are the main sources of soft X-ray (SXR) emission near a flare maximum and during the decay phase. In order to investigate the energy balance of the kernels it is necessary to have reliable estimates of the plasma density inside the kernels. A "standard" method of determining the electron number density, N, consists of a few steps.

i) Usually, the temperature, T, is estimated from the ratio of SXR fluxes measured with two different filters:

$$\frac{f_1(\bar{T})}{f_2(\bar{T})} = \frac{F_1}{F_2}, \tag{1}$$

where F_1 and F_2 are measured X-ray fluxes, $f_i(T)$ are response functions for measurements with two filters ($i = 1, 2$) and $\bar{T}$ is the estimated value of the temperature. In the case of observations with the *Reuven Ramaty High Energy Solar Spectroscopic Imager* (RHESSI, Lin *et al.*, 2002) the temperature is estimated from the slope of the SXR spectrum.

Flare kernels are multithermal (non-isothermal), *i.e.*

$$F_i = \int \varphi(T) f_i(T)\, \mathrm{d}T, \tag{2}$$

where $\varphi(T)$ is the differential emission measure (DEM). Therefore, the values of $\bar{T}$ obtained depend on the instrumental response functions $f_i(T)$, and we obtain different values of $\bar{T}$ from measurements with different instruments (see Table 1).

ii) Next, the emission measure is calculated using the formula

$$\mathrm{EM} = F_i / f_i(\bar{T}). \tag{3}$$

In many cases the response function, $f_i(T)$, steeply depends on temperature. Then random errors in the determination of the mean temperature, $\bar{T}$, may cause significant errors in EM. To improve this standard method of EM determination, we recommend that observations having flat response functions (low $|\mathrm{d}f_i/\mathrm{d}T|$ in the investigated range of temperatures) should be used to determine EM from Equation (3) (see Section 2). Then we have

$$F_i = \int \varphi(T) f_i(T)\, \mathrm{d}T \approx \bar{f}_i \int \varphi(T)\, \mathrm{d}T = \bar{f}_i \mathrm{EM}, \tag{4}$$

i.e. we will obtain reliable EM from Equation (3), despite that the emitting plasma is multithermal.

iii) The electron number density is estimated as

$$N = \sqrt{\mathrm{EM}/V}, \tag{5}$$

where V is the volume of emitting plasma. In order to estimate the volume V, it is necessary to assume the extent of the emitting plasma along the line of sight. This introduces significant uncertainty into the estimates of electron density calculated from Equation (5). The uncertainty is high when the shape of a flare kernel is elongated (elliptical) or irregular, since then it is most difficult to estimate what the extent of the emitting plasma along the line of sight is.

An additional drawback of the standard method of the determination of the density is due to the fact that it gives values averaged over the whole volume of a kernel. In reality, the emitting plasma can have a higher density if it occupies only a part of the kernel volume, *i.e.* if its filling factor is smaller than 1.

In our previous paper (Bąk-Stęślicka and Jakimiec, 2005, hereafter Paper I) we have proposed a new method of electron density determination

i) in which it is not necessary to assume the extent of the emitting plasma along the line of sight and
ii) which gives actual values of the electron density of the emitting plasma.

Rosner, Tucker, and Vaiana (1978) investigated models of steady-state coronal loops and they have found a "scaling law" of these models which can be written in the form

$$N_{\mathrm{SS}} = 2.1 \times 10^6 T^2/L, \tag{6}$$

where T is the temperature at the top of a loop, L is the semilength of the loop and N_{SS} is the electron number density within the loop.

Those authors have found that Equation (6) is also valid for hot "post-flare loops" having temperatures up to 10 MK (see their Figure 9b). The latter finding has been explained by Jakimiec *et al.* (1992), who carried out hydrodynamic modelling of the evolution of hot flaring loops. They have found that if the heating rate, $E_{\mathrm{H}}(t)$, of a flaring loop decreases slowly during the decay phase, the loop evolution can be described with a sequence of steady-state models [quasi-steady-state (QSS) evolution] and that Equation (6) is valid during this evolution. Therefore, Equation (6) can be used to determine densities N during a QSS evolution. The aim of the present paper is:

i) to improve the two methods of determination of the density, and
ii) to compare the densities obtained with the two methods.

We have selected a number of flares which showed QSS evolution during the decay phase. For these flares the electron density, N, has been derived by means of the standard method and with our QSS method. Comparison of the N values obtained with the two different methods allowed us: to test the obtained densities, and to evaluate the volume filling factor of the SXR emitting plasma.

Observations and their analysis are described in Section 2. Section 3 contains a summary and our conclusions.

2. Observations and Their Analysis

A long time ago it has been shown that it is useful to display flare evolution in temperature–density diagnostic diagrams (Jakimiec *et al.*, 1987, 1992). In such diagrams the QSS branch of the evolution of the flare is a straight line of inclination $\zeta = \mathrm{d}\log T/\mathrm{d}\log N \approx 0.5$. Soft X-ray images show that the size of the loop-top sources does not change significantly during the decay phase of many flares (*i.e.* their volume $V \approx$ const). Therefore, as we showed in Paper I, simplified diagnostic diagrams (where $\log N$ is replaced by $\log\sqrt{\mathrm{EM}}$), derived from GOES (*Geostationary Operational Environmental Satellites*) observations, are very useful for the detection of QSS evolution (see Figure 1). The correct inclination, $\zeta \approx 0.5$, of the QSS branch in these diagrams indicates that the temperature, T_{GOES}, derived from GOES

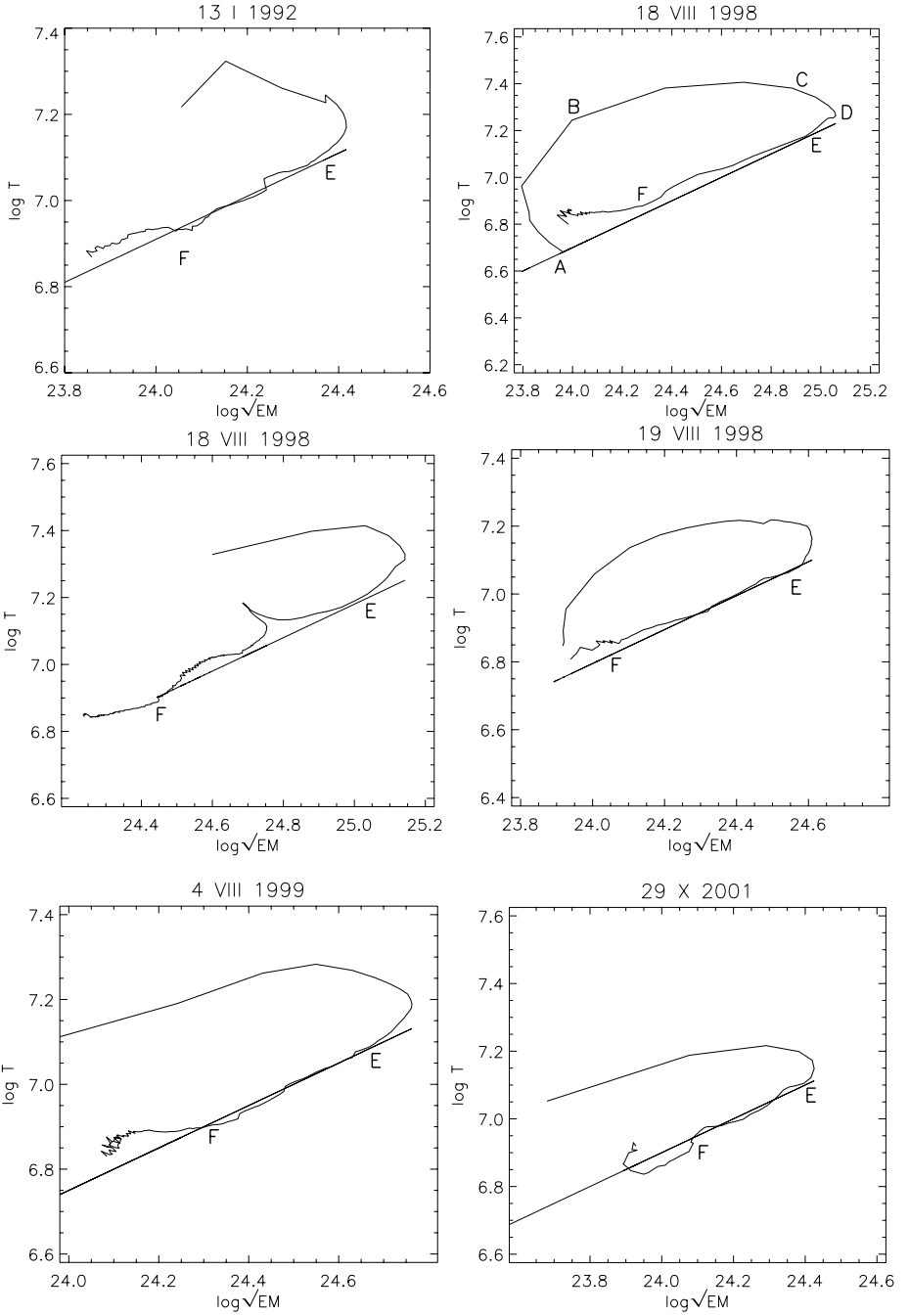

Figure 1 Examples of diagnostic diagrams ($\log \sqrt{\mathrm{EM}}$ *vs.* $\log T$; see the text for details) obtained from GOES data. The flare evolution proceeds from A to F. EF is the QSS branch. Straight lines have an inclination of $\zeta = 0.5$.

Table 1 List of selected flares.

	Date	GOES class	GOES max. (UT)	Beginning of the QSS evolution							
				Start (UT)	T_{SXT} (MK)	T_{GOES} (MK)	N_{SXT}	ΔN_{SXT}	N_{SS}	ΔN_{SS}	k
1	1991 Nov. 04	M3.4	23:23	23:47	8.0	11.5	7.1	1.4	12.6	2.5	0.6
2	1991 Nov. 19	C8.5	09:32	09:36	8.0	11.3	9.6	1.9	10.4	2.1	0.9
3	1991 Dec. 03	X2.2	16:39	16:40	10.4	19.1	75.6	15.1	84.7	16.9	0.9
4	1992 Jan. 13	M2.0	17:34	17:41	8.2	12.8	11.9	2.4	15.5	3.1	0.8
5	1992 Sep. 09	M3.1	02:13	02:15	9.2	14.0	19.6	3.9	27.3	5.5	0.7
6	1992 Oct. 04	M2.4	22:27	22:31	8.1	12.5	14.9	3.0	20.3	4.1	0.7
7	1992 Nov. 22	M1.6	23:10	23:11	9.0	13.3	20.1	4.0	39.2	7.8	0.5
8	1993 Jan. 02	C8.4	23:52	23:59	7.7	9.1	7.2	1.4	9.0	1.8	0.8
9	1993 Mar. 23	M2.3	01:53	02:11	8.3	10.7	4.4	0.9	4.2	0.8	1.0
10	1994 Jan. 16	M6.1	23:25	23:35	9.0	12.3	30.4	6.1	20.4	4.1	1.5
11	1998 Aug. 18	X2.8	08:24	08:31	10.9	15.6	40.5	8.1	30.1	6.0	1.3
12	1998 Aug. 18	X4.5	22:15	22:27	11.1	17.1	54.1	10.8	30.0	6.0	1.8
13	1998 Aug. 19	M3.0	14:26	14:50	8.0	10.3	14.9	3.0	6.8	1.4	2.2
14	1998 Nov. 22	X3.7	06:42	06:45	11.2	16.5	38.1	7.6	52.7	10.5	0.7
15	1998 Nov. 22	X2.5	16:23	16:28	12.3	16.3	35.5	7.1	34.5	6.9	1.0
16	1998 Nov. 23	X2.2	06:44	06:57	11.3	15.3	27.4	5.5	26.5	7.3	1.0
17	1999 Aug. 04	M6.0	05:57	06:09	8.5	12.9	17.4	3.5	22.0	4.4	0.8
18	2000 Jan. 12	M1.1	20:49	20:57	8.1	10.6	8.1	1.6	11.4	2.3	0.7
19	2000 Jun. 23	M3.0	14:31	14:42	9.0	12.3	14.0	2.8	10.1	2.0	1.4
20	2001 Oct. 29	M1.3	01:59	02:01	8.3	13.2	18.5	3.7	38.4	7.7	0.5

Values of N_{SXT} and N_{SS} are in 10^{10} cm^{-3}, $k = N_{SXT}/N_{SS}$, ΔN are 20% random errors (see text).

observations, adequately represents the mean temperature of the emitting plasma during the QSS flare evolution, and therefore we use this temperature in Equation (6).

In Paper I we have also found that the temperatures T_{SXT} are usually lower than T_{GOES} (SXT is the *Yohkoh*/Soft X-ray Telescope; see Tsuneta *et al.*, 1991). This is due to the fact that SXT has a narrower spectral range of sensitivity (1 – 5 keV for Be + Al12 filters; 1.6 – 25 keV for GOES). Low values of T_{SXT} result in a low inclination ($\zeta < 0.5$) of the QSS branch derived with this temperature (see Kołomański *et al.*, 2002 and our Paper I).

2.1. Comparison of the Electron Densities Obtained with Two Independent Methods

Using *Yohkoh*/SXT and GOES observations we have selected 20 flares which are limb or near-the-limb flares and their GOES diagnostic diagrams show a clear QSS branch. For the beginning of the QSS branch (near point E in Figure 1) we have determined the temperatures, T_{SXT} and T_{GOES}, and densities, N_{SXT} and N_{SS}, using SXT images and GOES data. The flaring loop semilength, L, has been calculated as $L = \frac{\pi}{2}h$, where h is the loop height measured in the SXR image. The values obtained of the temperatures and densities are given in Table 1. A comparison of N_{SXT} and N_{SS} is shown in Figure 2. We see good agreement between the N_{SXT} and N_{SS} values. The regression line is $N_{SXT} = 0.803N_{SS} + 3.13$ [this line is $N_{SXT} = 0.784N_{SS} + 2.21$ if we neglect the point (30, 54) which shows large deviation – see the discussion below]. The correlation coefficient is $r = 0.844$.

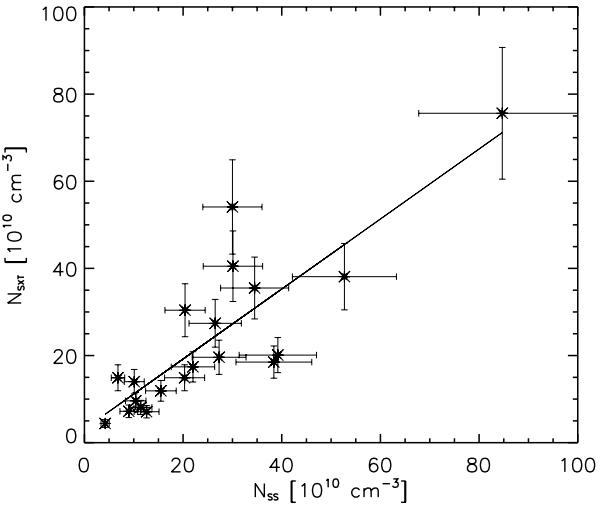

Figure 2 Comparison of N_{SXT} and N_{SS} for 20 selected flares. The straight line is the regression line: $N_{SXT} = 0.803 N_{SS} + 3.13$. Error bars are overplotted on each data point. Estimates of random errors are also given in Table 1.

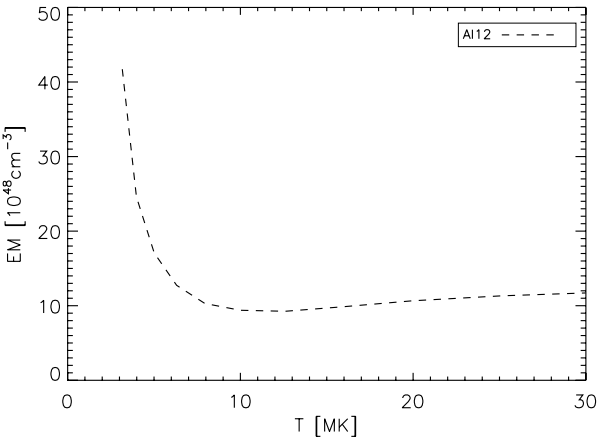

Figure 3 EM for various values of temperature for *Yohkoh*/SXT. The calculations have been carried out for a constant value of the SXR flux, F_i, measured with the Al12 filter ($F_i = 1.5 \times 10^6$ DN).

The good agreement between N_{SXT} and N_{SS} values shows that both methods of density determination give reliable values of the density (no large systematic errors in their calibration).

It is surprising that we obtain an agreement for the densities, despite significant systematic differences between the temperatures T_{SXT} and T_{GOES}. The explanation of this paradox is the following: The response function $f_i(T)$ for *Yohkoh*/SXT with Al12 filter changes only a little over a wide range of temperature, $T \approx 8-40$ MK [see curve f in Figure 9 in Tsuneta *et al.*, 1991]. Therefore, the emission measure, calculated according to Equation (3), only weakly depends on the temperature $\bar{T}$. To illustrate this effect, we have assumed a constant value of the X-ray flux, F_i, and calculated EM for various values of temperature (Figure 3). For the Al12 filter the dependence of EM on T is weak in the range of the flare temperatures. The dependence of the electron density, N_{SXT}, on temperature is even weaker, since $N_{SXT} \sim \sqrt{EM}$. This explains why we obtain correct values of N_{SXT}, despite the fact that T_{SXT} and $|dT_{SXT}/dt|$ are systematically too low.

Figure 3 displays the function $1.5 \times 10^6[\mathrm{DN}]/f_i(T)$ for SXT observations with Al12 filter. We have calculated the values of this function for T_{SXT} values, which are presented in Table 1. From these values of the function we obtained its mean value and random (r.m.s.) error. This gives the following form of Equation (3):

$$\mathrm{EM}[10^{48}\ \mathrm{cm}^{-3}] = (6.48 \pm 0.27) \times 10^{-6} F_i[\mathrm{DN}], \tag{7}$$

which does not depend on an estimated value of the mean temperature $\bar{T}$, provided that $\bar{T} \geq 8$ MK (DN is the Data Number in the *Yohkoh*/SXT observations). However, the coefficient in Equation (7) may slowly change with time due to a slow change in the sensitivity of the instrument.

In Table 1 it can be seen that most flares in our sample were strong ones (GOES class M and X). The electron number density, measured near SXR flare maximum, for most of the flares falls within the limits of $(4-50) \times 10^{10}\ \mathrm{cm}^{-3}$. But for one flare [No. 3 in Table 1, point (85, 76) in Figure 2], the density was extremely high, $N \approx 8 \times 10^{11}\ \mathrm{cm}^{-3}$. This high density has been obtained with both methods of density determination. The SXR image of this flare is shown in Figure 4. We see that it was a low flaring loop with very bright, compact loop-top kernel (at the beginning of the QSS evolution the diameter of the kernel was about 6000 km). This flare was also very strong in HXRs during its impulsive phase (about 1300 counts/s/SC in the *Yohkoh*/HXT 23 – 33 keV light curves, SC is a subcollimator).

The main source of random errors (deviations from the regression line in Figure 2) in the standard method of density determination from SXR images is the assumed extent of an SXR kernel along the line of sight. The main source of random errors in the QSS method of density determination is the uncertainty in estimates of the flaring-loop semilength, L. Estimates of L are usually based on the assumption that the shape of the loop is semicircular and (in the case of limb flares) that the loop lies in the plane of the image. Deviations from these assumptions are the main source of random errors in the QSS method of determination of the electron density.

Next we have calculated values of the ratio $k = N_{\mathrm{SXT}}/N_{\mathrm{SS}}$. The values of the ratio k are given in Table 1 and their distribution is shown in Figure 5. We see that for two flares (No. 12 and 13) the values of k are the highest ($k = 1.8$ and 2.2). SXR images of these two flares are shown in Figure 6. We see that their SXR kernels are elongated. The volumes, V, of such kernels were calculated under the assumption that they have "sausage-like" shape, *i.e.* that they are ellipsoids with semiaxes $a \times b \times b$. The high values of the ratio k suggest that the actual volume of the SXR emitting plasma is significantly larger, *i.e.* the third semiaxis is larger than b. This indicates that estimates of N_{SXT} for such elongated kernels can be loaded with the highest random errors. Therefore, we have excluded these two large values of k from the calculation of the mean value $\bar{k}$. We have obtained

$$\bar{k} = 0.88, \qquad s = \pm 0.28, \tag{8}$$

where s is random (r.m.s.) error of a single estimate of k.

In Figure 5 we see that k-values are concentrated around this mean value. The value of $\bar{k}$, which is close to 1, confirms the good agreement of N_{SXT} and N_{SS} values. We see that random (r.m.s.) error, s, of k-values is about 30%. Assuming that the contribution of random errors of N_{SXT} and N_{SS} to this random error of k are similar in size, we conclude that the random error of a single determination of N_{SXT} or N_{SS} is about $30\%/\sqrt{2} \approx 20\%$.

The values of N_{SXT}, obtained with the standard method, are the mean electron number densities averaged over the SXR-kernel volume. But the QSS method of determination of the density provides the actual density of the emitting plasma. Therefore, the ratio $k =$

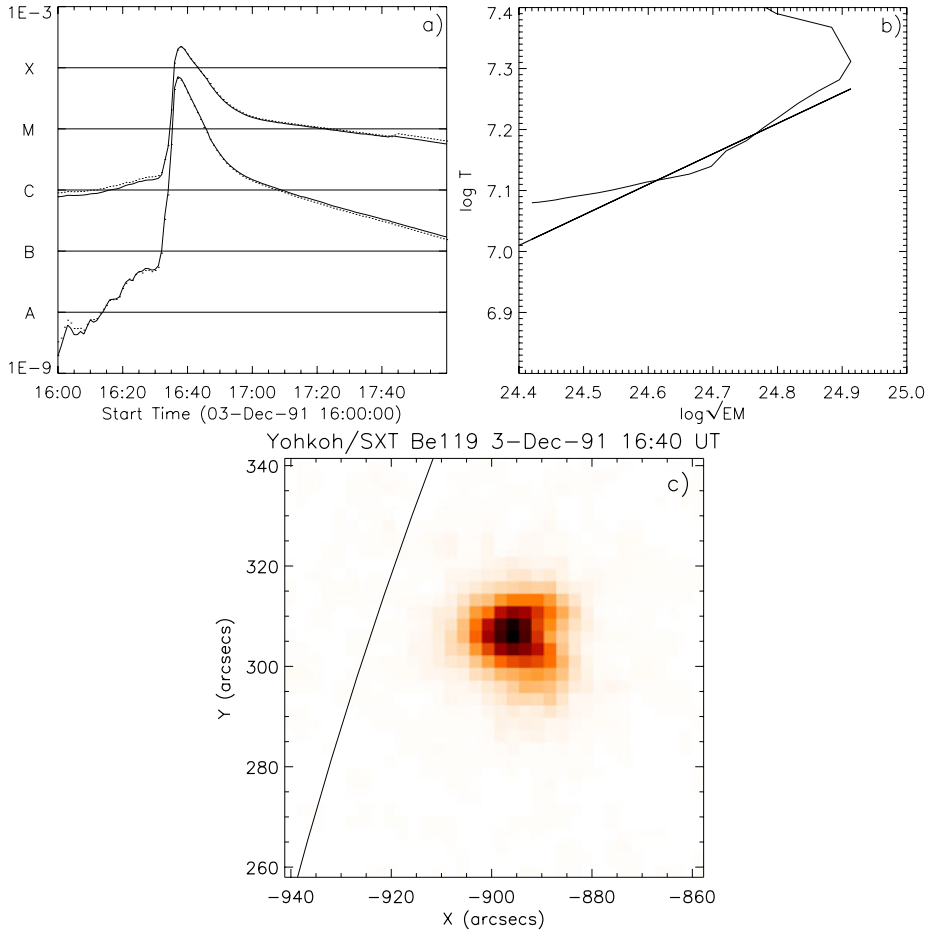

Figure 4 (a) GOES light curve, (b) diagnostic diagram, and (c) sample SXT(Be119) image (inverse intensity scale in colour) of the 3 December 1991 flare (the solid line shows the solar limb).

$N_{\mathrm{SXT}}/N_{\mathrm{SS}}$ provides an estimate of the fraction of the kernel's volume which is filled with the SXR emitting plasma ("filling factor"). In Figure 5 we see that the k-values are concentrated around $k \approx 0.9$, which means that, typically, near the flare maximum the kernel's volume is nearly entirely filled with hot SXR emitting plasma. The remaining, $(1-k)$, fraction of the volume can be filled with plasma of lower temperature, $T < 4$ MK, whose contribution to the investigated SXR emission is marginal. Values $k > 1$ are due to random errors in both methods of determination of the density.

3. Summary and Conclusions

We have found that simplified diagnostic diagrams (T *vs.* $\sqrt{\mathrm{EM}}$), derived from GOES observations, are adequate to identify the quasi-steady-state (QSS) phase of flare evolution. The correct inclination, $\zeta \approx 0.5$, of the QSS branches in the diagnostic diagrams shows that the

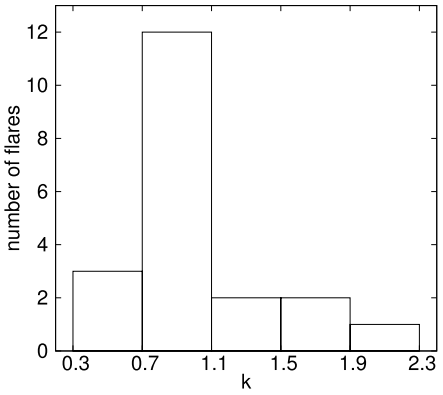

Figure 5 Histogram of the ratio $k = N_{SXT}/N_{SS}$ for 20 analysed flares.

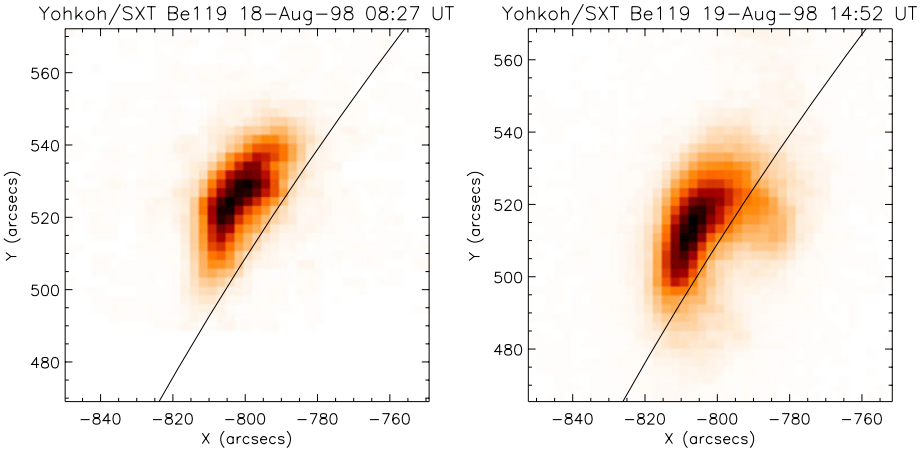

Figure 6 Sample SXT(Be119) images (inverse intensity scale in colour) of 18 August 1998 (left) and 19 August 1998 (right) flares.

temperature, T_{GOES}, derived from the GOES observations, adequately represents the mean temperature of the hot, SXR emitting plasma.

For the QSS branch of the flare evolution we were able to determine the electron number density, N, for SXR loop-top flare kernels, with two independent methods, which are described in Sections 1 and 2. Good agreement of the N-values obtained with the two methods confirms the reliability of the densities derived from the *Yohkoh*/SXT images. In Section 2, we have explained why we obtain correct N_{SXT} electron densities, despite the fact that the *Yohkoh*/SXT temperatures are systematically too low.

We have obtained that the electron density near the SXR flare maximum falls within the limits of $(4-50) \times 10^{10}$ cm^{-3}, but in one case of a strong, compact flare it was extremely high, $N \approx 8 \times 10^{11}$ cm^{-3}.

The densities, N_{SXT}, derived from the SXR images, are mean electron densities averaged over SXR flare kernels. But the densities, N_{SS}, obtained with the second (QSS) method, provide actual densities of the emitting plasma. Therefore, the ratio N_{SXT}/N_{SS} provides an estimate of the filling factor of the kernel with hot, SXR emitting plasma. Our analysis of

the k values obtained shows that, typically, flare kernels near SXR flare maximum are nearly entirely filled with hot, SXR emitting plasma.

Acknowledgements The *Yohkoh* satellite is a project of the Institute of Space and Astronautical Science of Japan. GOES is a satellite of National Oceanic and Atmospheric Administration (NOAA), USA. We thank the anonymous referee for useful comments and suggestions. This investigation has been supported by grant N203 1937 33 from the Polish Ministry of Science and High Education.

References

Bąk-Stęślicka, U., Jakimiec, J.: 2005, *Solar Phys.* **231**, 95.

Jakimiec, J., Sylwester, B., Sylwester, J., Lemen, J.R., Mewe, R., Bentley, R.D., Peres, G., Serio, S., Schrijver, J.: 1987, In: Stepanov, V.E., Obridko, V.N. (eds.) *Solar Maximum Analysis*, VNU Science Press, Utrecht, 91.

Jakimiec, J., Sylwester, B., Sylwester, J., Serio, S., Peres, G., Reale, F.: 1992, *Astron. Astrophys.* **253**, 269.

Kołomański, S., Jakimiec, J., Tomczak, M., Falewicz, R.: 2002, *Adv. Space Res.* **30**(3), 665.

Lin, R.P., Dennis, B.R., Hurford, G.J., Smith, D.M., Zehnder, A., Harvey, P.R., *et al.*: 2002, *Solar Phys.* **210**, 3.

Rosner, R., Tucker, W., Vaiana, G.: 1978, *Astrophys. J.* **220**, 643.

Tsuneta, S., Acton, L., Bruner, M., Lemen, J., Brown, W., Caravalho, R., Catura, R., Freeland, S., Jurcevich, B., Owens, J.: 1991, *Solar Phys.* **136**, 37.